

Stable fetal cardiomyocyte grafts in the hearts of dystrophic mice and dogs.

G Y Koh, ... , D P Zipes, L J Field

J Clin Invest. 1995;96(4):2034-2042. <https://doi.org/10.1172/JCI118251>.

Research Article

This report documents the formation of stable fetal cardiomyocyte grafts in the myocardium of dystrophic dogs. Preliminary experiments established that the dystrophin gene product could be used to follow the fate of engrafted cardiomyocytes in dystrophic mdx mice. Importantly, ultrastructural analyses revealed the presence of intercalated discs consisting of fascia adherens, desmosomes, and gap junctions at the donor-host cardiomyocyte border. To determine if isolated cardiomyocytes could form stable intracardiac grafts in a larger species, preparations of dissociated fetal canine cardiomyocytes were delivered into the hearts of adult CXMD (canine X-linked muscular dystrophy) dogs. CXMD dogs, like Duchenne muscular dystrophy patients and mdx mice, fail to express dystrophin in both cardiac and skeletal muscle. Engrafted fetal cardiomyocytes, identified by virtue of dystrophin immunoreactivity, were observed to be tightly juxtaposed with host cardiomyocytes as long as 10 wk after engraftment, the latest date analyzed. Confocal laser scanning microscopy revealed the presence of connexin43, a major constituent of the gap junction, at the donor-host cardiomyocyte border. The presence of intracardiac grafts was not associated with arrhythmogenesis in the CXMD model. These results indicate that fetal cardiomyocyte grafting can successfully augment cardiomyocyte number in larger animals.

Find the latest version:

<https://jci.me/118251/pdf>



Stable Fetal Cardiomyocyte Grafts in the Hearts of Dystrophic Mice and Dogs

Gou Young Koh,* Mark H. Soonpaa,* Michael G. Klug,* Harald P. Pride,* Barry J. Cooper,† Douglas P. Zipes,* and Loren J. Field*

*Krannert Institute of Cardiology, Indiana University School of Medicine, Indianapolis, Indiana 46202-4800; and †Department of Pathology, New York State College of Veterinary Medicine, Cornell University, Ithaca, New York 14853-6401

Abstract

This report documents the formation of stable fetal cardiomyocyte grafts in the myocardium of dystrophic dogs. Preliminary experiments established that the dystrophin gene product could be used to follow the fate of engrafted cardiomyocytes in dystrophic mdx mice. Importantly, ultrastructural analyses revealed the presence of intercalated discs consisting of fascia adherens, desmosomes, and gap junctions at the donor-host cardiomyocyte border. To determine if isolated cardiomyocytes could form stable intracardiac grafts in a larger species, preparations of dissociated fetal canine cardiomyocytes were delivered into the hearts of adult CXMD (canine X-linked muscular dystrophy) dogs. CXMD dogs, like Duchenne muscular dystrophy patients and mdx mice, fail to express dystrophin in both cardiac and skeletal muscle. Engrafted fetal cardiomyocytes, identified by virtue of dystrophin immunoreactivity, were observed to be tightly juxtaposed with host cardiomyocytes as long as 10 wk after engraftment, the latest date analyzed. Confocal laser scanning microscopy revealed the presence of connexin43, a major constituent of the gap junction, at the donor-host cardiomyocyte border. The presence of intracardiac grafts was not associated with arrhythmogenesis in the CXMD model. These results indicate that fetal cardiomyocyte grafting can successfully augment cardiomyocyte number in larger animals. (*J. Clin. Invest.* 1995; 96:2034–2042.) Key words: myocardial repair • gene therapy • cardiomyopathy • muscular dystrophy

Introduction

It is generally believed that the proliferative capacity of the adult mammalian myocardium is limited. Consequently cardiomyocyte loss resulting from injury or disease is essentially irreversible. The ability to augment cardiomyocyte number might

therefore be of therapeutic value, provided that the new myocytes functionally integrate with the pre-existing myocardium.

One potential approach to augment myocyte number in the adult heart entails the direct engraftment of isolated muscle cells. It is now established that several types of myocytes can be stably introduced into the adult murine myocardium. For example, AT-1 tumor cardiomyocytes (a differentiated tumor cell lineage derived from transgenic mice which expressed the SV-40 large T-antigen oncogene in the myocardium) formed stable intracardiac grafts in the hearts of syngeneic adult animals (1). The usefulness of AT-1 cardiomyocytes for long-term engraftment studies is dramatically limited due to their transformed phenotype. C2C12 myoblasts have also been used to generate cardiac grafts (2–4). Engrafted C2C12 myoblasts rapidly withdrew from the cell cycle and fused to form myotubes (2). Although the nascent myotubes were observed to be aligned with host myocardial fibers, the potential for functional coupling between host and donor myocytes is currently unknown. More recently, fetal murine cardiomyocytes were used to form stable grafts in the adult heart (5). These experiments relied on the use of transgenic mice (designated MHC-nLAC) which expressed a nuclear localized β -galactosidase (β GAL)¹ reporter gene in cardiac myocytes. The fate of engrafted donor cells was tracked by virtue of the transgene-encoded β GAL activity. While desmosomes were observed to connect donor cells with the host myocardium, the presence of nascent gap junctions could not be established unequivocally. The fetal cardiomyocyte grafts were not arrhythmogenic, and were present for as long as 6 mo (5).

Although these studies collectively demonstrated that augmentation of myocyte number in the adult murine heart is feasible, it was not clear if the process would be equally successful in larger species. The importance of this caveat is underscored by results obtained with myoblast transfer into skeletal muscle beds: although the procedure worked well in murine systems (6–8), results obtained to date in humans and dogs have been relatively disappointing (9–11).

As indicated above, fetal cardiomyocyte engraftment experiments require a reliable marker with which to follow the fate of donor cells. The initial studies in mice utilized a cardiomyocyte-specific β GAL transgene reporter. Unfortunately the use of analogous transgene reporters in larger species more amenable to interventional cardiovascular experimentation and functional

G. Y. Koh, M. H. Soonpaa, and M. G. Klug contributed equally to this manuscript.

Address correspondence to Loren J. Field, Krannert Institute of Cardiology, 1111 West 10th Street, Indianapolis, IN 46202-4800. Phone: 317-630-7776; FAX: 317-274-9697.

Received for publication 3 April 1995 and accepted in revised form 20 July 1995.

analyses is fiscally and experimentally impractical. A series of murine experiments was therefore initiated to determine if naturally occurring polymorphisms or mutations could be exploited to follow the fate of engrafted fetal cardiomyocytes. The dystrophin gene product was selected because it is expressed at high levels in cardiac as well as skeletal muscle. These studies served as a direct prelude for experiments in larger species, as both murine and canine models lacking the dystrophin gene product are available.

The results reported here indicate that the dystrophin gene product can be reliably used to monitor the fate of engrafted fetal cardiac myocytes in dystrophic mdx mice. Nascent intercalated discs comprised of desmosomes, fascia adherens, and gap junctions were observed to connect host and donor cardiomyocytes in the murine model. Analogous experiments using canine X-linked muscular dystrophy (CXMD) dogs, a canine model of Duchenne muscular dystrophy, indicated that fetal cardiomyocyte engrafting was readily extended to larger species more amenable to physiologic characterization. Connexin43 immunoreactivity was observed at donor-host cardiomyocyte borders, suggesting the formation of gap junctions. Importantly, the presence of fetal cardiomyocyte grafts in the canine myocardium did not predispose the host animals to overt arrhythmogenic episodes. The implications of these results with respect to the potential for therapeutic cardiac grafting is discussed.

Methods

Mouse cardiomyocyte grafting. Single cell preparations of transgenic fetal donor cardiomyocytes were prepared and injected into the left ventricular wall of dystrophic [C3HeB/FeJ × C57B1/10ScSn-mdx/J]F₁ males essentially as described previously (5). Briefly, females with 15-d embryos (onset of pregnancy determined by vaginal plugs) were sacrificed by cervical dislocation. Embryos were removed, decapitated, and hearts were harvested under PBS, and ventricles and atria were separated. Transgenic ventricles (identified by cardiac βGAL activity) were digested in 0.1% collagenase (Worthington) in DPBS (Dulbecco's phosphate-buffered saline; Sigma Chemical Co., St. Louis, MO) for 45 min, and were triturated with a Pasteur pipette in PC-1 medium (Ventrex, Coons Rapids MN) with 10% FBS, resulting in a suspension of single cells. Immediately after isolation, fetal cardiomyocytes were washed three times with DPBS and directly injected into the ventricular myocardium of syngeneic host animals under open heart surgery as described (5). 1–10 × 10⁴ cells were injected in a volume of 2–3 μl using a plastic syringe fitted with a 30-gauge needle. C3HeB/FeJ and C57B1/10ScSn-mdx/J mice were obtained from the Jackson Laboratory (Bar Harbor MA).

Canine cardiomyocyte grafting. Third trimester mongrel dogs were sedated 20 min before surgery with 1 mg Butorphanol (intramuscular). Anesthesia was then induced using Thiopental Sodium (intravenous) at 25 mg/kg. The dogs were intubated and placed on the surgical table in a left lateral recumbency. Anesthesia was maintained with Isoflurane (2% vaporized in oxygen delivered at 2 liters/min). Fetuses were delivered by Caesarean-section, heparinized (10,000 U/kg intraperitoneal), and the hearts removed and single cell suspensions of cardiomyocytes prepared by retrograde collagenase perfusion on a Langendorff apparatus as previously described (12). Isolated cells were rinsed once with DME supplemented with 20% FBS, and then three times with serum-free DME before engraftment. For engraftment, CXMD dogs (6–9 mo old) were sedated and anesthetized as described above. The dogs were prepared for surgery, and the chest opened in layers at the fifth intercostal space. The left lung was reflected away from the heart, the pericardial fat dissected, and a 5-cm incision made in the pericardium. After the fetal cardiomyocytes were delivered, a vacuum tube was placed in the thoracic cavity to remove blood and fluids. The chest was closed in

layers using continuous and/or interrupted suturing, the skin was closed with skin staples and air in the thoracic cavity was evacuated using the Valsalva technique. The dogs were gradually weaned from the gas anesthetic agent by progressively reducing the Isoflurane flow rate to zero, and then challenged to begin independent respiration. To block graft rejection, dogs were treated daily with cyclosporine (15 mg/kg) and corticosteroid (2 mg/kg), starting 1 d before engraftment. After one week, the treatment was reduced to alternating days for the duration of the study.

Immunohistologic analysis of fetal cardiomyocyte grafts. After sacrifice, engrafted hearts were dissected, cryoprotected in 30% sucrose, embedded and sectioned at 10 μm using standard histologic techniques (13). For anti-dystrophin immunohistology (murine and canine grafts), sections were incubated with CAP 6-10 (gift of Dr. T. Byers, Indiana University) or DYS1 (Novocastra Laboratories, Newcastle upon Tyne, UK) in 1 × PBS, 1% BSA for 24 h at 4°C, rinsed and reacted with a rhodamine conjugated secondary antibody. For anti-utrophin immunohistology (canine grafts), sections were incubated with monoclonal antibody DRP2 (which recognizes the utrophin isoform which is upregulated in dystrophic tissue, Novocastra Laboratories) in 1 × PBS, 1% BSA for 60 min at room temperature, rinsed, and signal was amplified with the biotin-streptavidin system using a FITC conjugate. For X-GAL (5-bromo-4-chloro-3-indolyl-β-D-galactoside) staining (murine grafts), sections were postfixed in acetone:methanol (1:1) and overlaid with 1 mg/ml X-GAL, 5 mM potassium ferricyanide, 5 mM potassium ferrocyanide and 2 mM magnesium chloride in PBS. Sections were then counterstained with H and E according to manufacturer's specifications (Sigma Diagnostics, St. Louis MO). For anti-connexin43 staining (canine grafts), sections were reacted with MAB3068 (Chemicon International, Temecula CA) in 1 × PBS, 1% BSA for 24 hrs at 4°C. Sections were then reacted with a FITC-conjugated anti-mouse IgG secondary antibody.

Ultrastructural analysis of murine cardiac grafts. Engrafted mice were sacrificed by cervical dislocation, hearts were harvested and perfused on a Langendorff apparatus with 2% glutaraldehyde in 0.1 M cacodylate buffer (pH 7.4). After immersion fixation overnight in the same buffer, 200 μm coronal sections were made with a vibratome, and the engrafted regions identified by X-GAL as described above. Regions carrying fetal cardiomyocyte grafts were post-fixed in osmium tetroxide and stained en bloc with uranyl acetate. Dehydration and infiltration times were adjusted to minimize leaching of X-GAL reaction product while retaining adequate morphology. All remaining TEM protocols were as described previously (1, 2, 5).

Electrocardiographic analysis. Engrafted dogs were sedated and anesthetized as described above and placed on a surgical table in a supine recumbency. A 12 lead ECG was then recorded using a Marquette Electronics Mac 15 recorder (Milwaukee WI) with the leads attached to the animal in the standard 12 lead configuration: right foreleg, left foreleg, right hindleg, left hindleg and six chest leads.

Results

To determine if the dystrophin gene product could be used to monitor the fate of engrafted fetal cardiomyocytes, the MHC-nLAC transgene was crossed into a [C57B1/10SnJ × C3HeB/FeJ] F₁ background, and donor cardiomyocytes from the resulting transgenic animals were isolated at embryonic day 15. The donor cardiomyocytes expressed the dystrophin gene product as well as the transgene-encoded βGAL reporter (data not shown). Recipient animals were generated by crossing mdx (C57B1/10ScSn-mdx/J) females with C3HeB/FeJ males. Cardiomyocytes in the resulting male F₁ animals had a Xdys/Y genotype, did not express dystrophin, and were nontransgenic for the MHC-nLAC reporter (data not shown). By employing these crosses, the resulting host and donor cells were syngeneic. Donor cardiomyocytes were delivered to the left ventricular

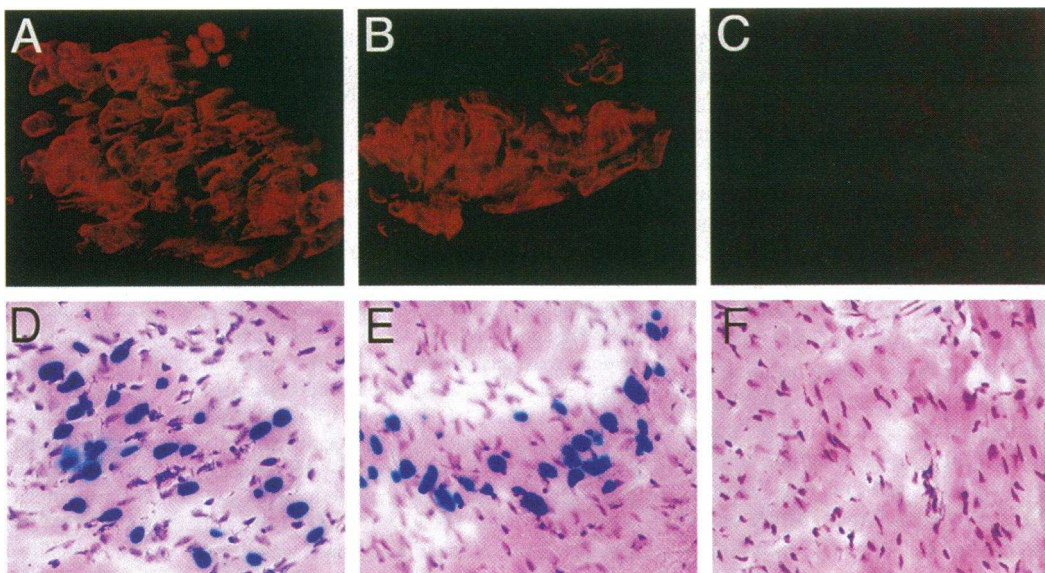


Figure 1. Murine fetal cardiomyocyte grafts in mdx hearts. (A and B) Anti-dystrophin immunostaining of fetal cardiomyocyte grafts in adult dystrophic hearts. Dystrophin positive (red fluorescence) fetal donor cardiomyocytes are readily seen. Host cardiomyocytes do not express dystrophin. (D and E) Histochemical analysis of sections adjacent to those depicted in A and B, respectively. Sections were stained with X-GAL, and then counter-stained with H and E. Engrafted fetal cardiomyocytes were identified by their dark blue nuclei, and exhibited a distribution similar to those localized by anti-dystrophin immunohistology of the adjacent sections depicted in A and B. Cardiomyocytes from the dystrophic host exhibited purple hematoxylin nuclear staining. (C and F) Anti-dystrophin immunohistological and X-GAL histochemical analyses, respectively, of non-engrafted control mdx myocardium. Note the absence of dystrophin immunoreactivity and β galactosidase activity. The histochemical section was counter-stained with H and E.

free wall in an open chest procedure as described previously (1, 5).

Immunohistologic analyses revealed the presence of dystrophin-positive donor cardiomyocytes within the dystrophin-negative host myocardium at one month post-engraftment (Fig. 1, A and B). Dystrophin positive cells were detected in approximately 60% ($n = 44$) of the animals receiving fetal cardiomyocyte injections, in agreement with previous results which relied on the MHC-nLAC reporter (5). To rule out the possibility that the observed dystrophin immunoreactivity was due to reversion at the dystrophin locus in host cardiomyocytes, adjacent sections were stained with X-GAL. The donor cardiomyocytes were easily identified by intense blue nuclear staining due to the β GAL reporter (Fig. 1, D and E). These data indicated that the dystrophin gene product could be used to follow the fate of engrafted fetal cardiomyocytes. As expected, neither dystrophin nor X-GAL signal could be detected in control sections of non-engrafted mdx myocardium (Fig. 1, C and F, respectively). Finally, it is of interest to note that although the overall distribution of dystrophin positive cells was similar to the distribution of X-GAL positive cells on adjacent sections (compare Fig. 1, A and B to D and E, respectively), the number of graft cells appeared greater with dystrophin staining. Since a 10- μ m section will undoubtedly miss a significant number of the nuclei present in the cardiomyocytes sampled, this discrepancy is simply an artifact of sectioning.

Although previous studies clearly identified the presence of desmosomes and fascia adherens between engrafted fetal cardiomyocytes and the host myocardium, the presence of gap junctions was not established (5). Collectively these three structures comprise the intercalated disc, a cardiomyocyte junctional complex which frequently exhibits a step-wise morphology con-

sisting of transverse and lateral regions. The desmosomes (intercellular contacts responsible for the propagation of contractile forces) and fascia adherens (cell membrane anchors for the terminal actin filaments of the myofibril) reside in the transverse region of the intercalated disc. The lateral area of the intercalated disc contains gap junctions, which are the electrical conduit for action potential propagation through the myocardium. The formation of gap junctions between donor and host myocardium is an absolute prerequisite for excitation-contraction coupling.

Engrafted mdx hearts were subjected to ultrastructural analyses to unequivocally establish the presence of gap junctions between donor and host cardiomyocytes. The fixation, staining and embedding procedures were optimized so as to retain satisfactory morphology while providing unambiguous identification of donor and host cells. Engrafted fetal cardiomyocytes were observed to be tightly juxtaposed with host cells (Fig. 2 A). As in previous studies (5), donor cardiomyocytes were identified by the presence of the X-GAL reaction product, which appeared as a perinuclear crystalloid deposit (Fig. 2 D, arrows). Host cardiomyocytes lacked the perinuclear crystalloid deposit (Fig. 2 B). Desmosomes and fascia adherens were observed in the transverse regions of an intercalated disc in low magnification micrographs (Fig. 2 A, arrows). Examination of high magnification micrographs revealed the presence of laminar structures on the lateral region of the intercalated disc (Fig. 2 C, arrows): this structural motif is diagnostic for gap junctions. Thus all of the physical attributes required for action potential and force propagation are present between the donor and host cardiomyocytes in the murine system.

To determine if the fetal cardiomyocyte grafting procedure could be extended to larger species, experiments were initiated

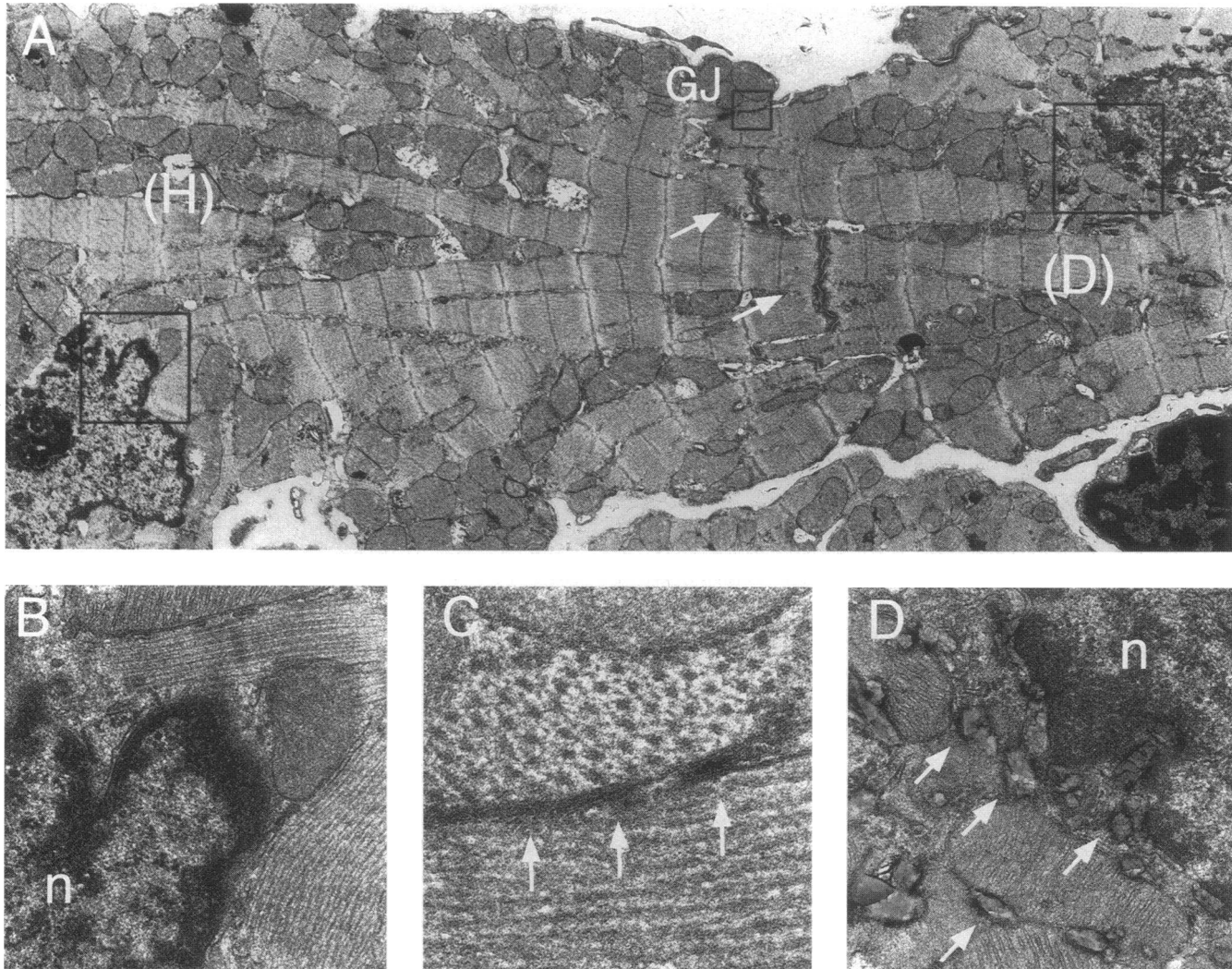


Figure 2. Nascent gap junctions between an engrafted fetal cardiomyocyte and a host cardiomyocyte. (A) Low power TEM micrograph of an mdx heart engrafted with fetal cardiomyocytes. A host cardiomyocyte is indicated by (H), while a fetal donor cardiomyocyte is indicated by (D). Arrows indicate an intercalated disc between the host and donor cells. Boxed region labeled GJ indicates the position of gap junctions on the lateral area of the intercalated disc. Note also the sarcomere alignment between the two cells. (B) High power view of the boxed region of the mdx host cardiomyocyte nucleus depicted in A. Note the absence of perinuclear crystalloid deposits. (C) High power view of gap junctions (boxed region labeled GJ in A). Note the laminar structure (arrows), which is diagnostic for identifying gap junctions in normal myocardial tissue. (D) High power view of the boxed region of the donor MHC-nLAC cardiomyocyte nucleus depicted in A. Note the presence of abundant perinuclear crystalloid deposits (arrows).

with CXMD dogs (14–17). Like Duchenne patients and mdx mice, CXMD dogs do not express dystrophin (14). As such, the dystrophin gene product could once again be used to follow the fate of engrafted cardiomyocytes. CXMD dogs were grafted with fetal cardiomyocytes isolated from early third trimester mongrel animals. In all cases, a portion of the fetal heart was subjected to immunohistologic analyses to ensure that the donor cells were dystrophin positive. The recipients were maintained on a regimen of cyclosporine and corticosteroid treatment to prevent graft rejection. Hearts were harvested at various times after implantation, and the engrafted region was dissected and processed for immunohistology using either the CAP 6-10 or DYS1 anti-dystrophin antibodies.

Phase contrast analysis of engrafted regions from CXMD hearts revealed a typical myocardial morphology exhibiting well-aligned cardiomyocytes (Fig. 3 A). Visualization of the

same field under fluorescence illumination indicated that a large number of these cardiomyocytes were dystrophin positive donor cells (Fig. 3 B). In contrast, no dystrophin signal was observed in regions of the myocardium which were not engrafted, consistent with the low reversion rate for this mutation. It should also be noted that the rare reversions which do occur in the CXMD myocardium invariably appear as isolated myocytes (B. J. Cooper, unpublished observation), rather than as the relatively large regions of dystrophin positive cells which were seen in the engrafted hearts (Fig. 3, B and C).

Additional immunohistologic analyses were performed with an anti-utrophin antibody. Utrophin, an autosomal homologue of the dystrophin locus, has been observed to be up-regulated in dystrophic muscle (18–20). Utrophin is also markedly up-regulated in the dystrophic CXMD myocardium as compared to the non-dystrophic canine heart (Fig. 3, E and F, respec-

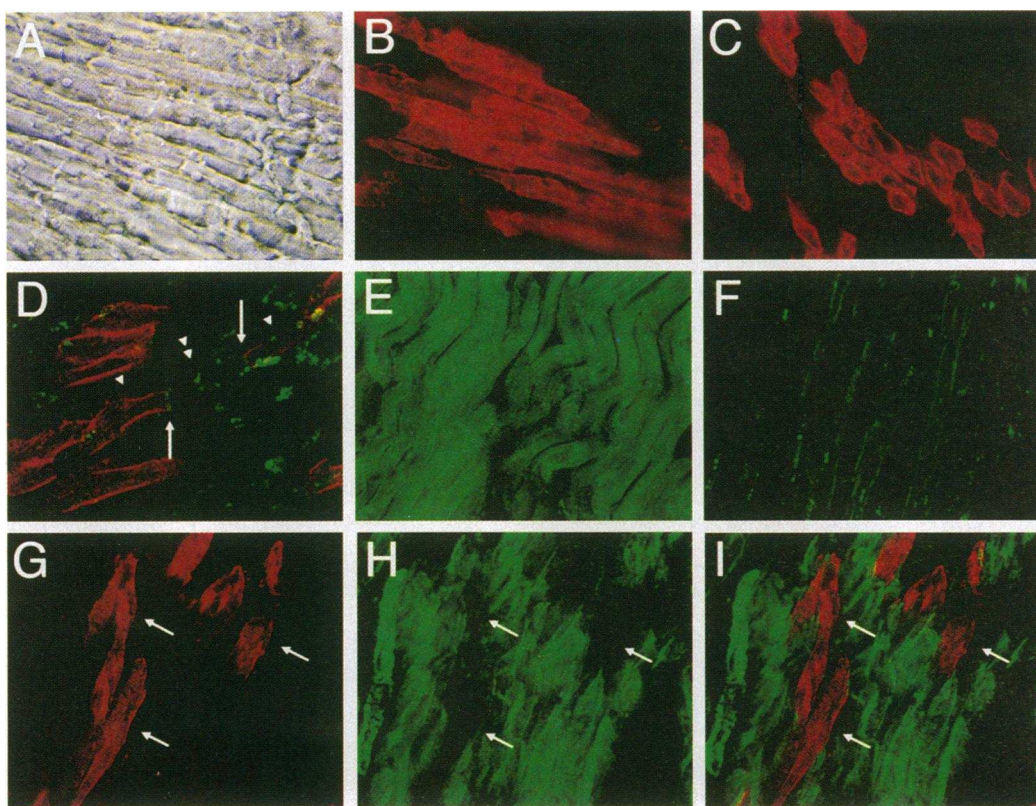


Figure 3. Fetal canine cardiomyocytes form stable grafts in CXMD hearts. (A) Phase contrast photomicrograph of an engrafted region of a CXMD heart. The heart depicted was harvested at 2.5 wk after engraftment; note the longitudinal alignment of all of the cells present in this field. (B) Anti-dystrophin immunofluorescence of the same field depicted in A. Note the presence of dystrophin positive donor cells (red fluorescence) which appear in longitudinal section. (C) Immunohistologic analysis of a second engrafted region from the same heart with anti-dystrophin antibody. In this case the engrafted cells (red fluorescence) were cut in cross section. (D) Confocal laser scanned image of an engrafted CXMD heart processed simultaneously for dystrophin (red fluorescence) and connexin43 (green fluorescence) immunohistology. Two engrafted fetal cardiomyocytes (red fluorescence, see arrow heads) are separated by a host cardiac myocyte (see double arrowhead). Connexin43 immunoreactivity (green fluorescence, see arrows) is present along the axial borders of the cells, suggesting the presence of intercalated discs. (E) Immunohistologic analysis of a CXMD heart with an anti-utrophin antibody. Note uniform utrophin immunoreactivity (green fluorescence) throughout the myocardium. (F) Immunohistologic analysis of a non-dystrophic heart with an anti-utrophin antibody. Note the absence of utrophin immunoreactivity in the myocardium. (G) Confocal image of dystrophin immunoreactivity (red fluorescence) of a CXMD heart engrafted with fetal cardiomyocytes. A group of donor cells is readily seen (arrows). (H) Confocal image of utrophin immunoreactivity (green fluorescence) of the same section depicted in G. Note the absence of utrophin immunoreactivity in the dystrophin-positive cells (arrows). (I) Simultaneous imaging of dystrophin (red fluorescence) and utrophin (green fluorescence) immunoreactivity in the same section depicted in G and H. Note the absence of yellow signal, indicating that dystrophin and utrophin immunoreactivity does not co-localize. In all cases, dystrophin immunoreactivity was confirmed with both the CAP 6-10 and the DYS1 antibodies on adjacent sections.

tively). The virtual absence of immunoreactivity in the non-dystrophic myocardium suggested that utrophin could be used as a second, albeit negative, marker for the engrafted cardiomyocytes. Engrafted regions from a CXMD heart were therefore examined simultaneously for dystrophin and utrophin expression using confocal microscopy. Anti-dystrophin immunohistology (red signal, Fig. 3 G, arrows) revealed the presence of a group of engrafted fetal cardiomyocytes. Although utrophin immunoreactivity was uniformly present in the host myocardium on the same section (green signal, Fig. 3 H), virtually no immunoreactivity was detected in the dystrophin positive graft cardiomyocytes (arrows). Visualization of both signals simultaneously (Fig. 3 I) confirmed the absence of dystrophin and utrophin co-localization, which would appear as a yellow signal in this assay. This observation is consistent with the absence of utrophin expression in the nondystrophic myocardium, and thus provides a second marker for the engrafted cardiomyocytes.

Engrafted regions of the CXMD hearts were also examined for connexin43 expression. Connexin43 is the major constituent of the cardiac gap junction (21). Confocal microscopy revealed the presence of a host cardiomyocyte aligned longitudinally between two donor cardiomyocytes, as evidenced by anti-dystrophin immunohistology (Fig. 3 D). Connexin43 immunoreactivity was apparent at junctional complexes between the donor and host cells, suggestive of the presence of coupling. Unfortunately the absence of a suitable histochemical stain for the canine donor cells precluded ultrastructural assessment of donor-host gap junction formation.

Successful rescue of damaged myocardium will require that the donor myocytes be seeded at a sufficiently high density to impact on myocardial function. Experiments were therefore initiated to estimate the percentage of cells which were dystrophin positive at a given site of injection. On average 37% of the cardiomyocytes in the immediate vicinity of the injection

Table I. Percent Donor Cardiomyocytes at Individual Injection Sites

Injection site	Area analyzed (mM ²)	DYS ⁺ cells	DYS ⁻ cells	Percent DYS ⁺ cells
A	0.3	125	71	63.7
B	0.2	52	188	20.8
C	0.1	18	17	51.4
D	0.1	38	52	42.2
E	0.35	168	297	36.1
F	0.05	12	49	19.7
G	0.1	29	79	26.9
Average		442	753	37.0

Values were obtained from a single plane of section, and thus do not represent the total number of cells stably delivered to the site.

site displayed dystrophin immunoreactivity (Table I), although the absolute values varied between individual sites (ranging from 20% to 60%). Importantly, as many as 168 dystrophin positive cells could be detected in a single section of an injection site. Additional experiments indicated that dystrophin positive grafts could be detected when 10⁴ through 10⁶ donor cardiomyocytes were delivered to a single site (Table II). Furthermore, the myocardium could readily accommodate multiple injections of donor cardiomyocytes within a relatively confined area (Table II). Optimization of these variables undoubtedly will impact on the number of cardiomyocytes which can be engrafted at a given site.

Surface electrocardiographic analysis of engrafted mdx mice failed to detect overt graft-induced arrhythmias, in agreement with previous observations (1, 2, 5). However, the relatively small size and rapid rate of the mouse heart might render these animals resistant to arrhythmia. In contrast, the utility of canine models for the assessment of cardiac arrhythmia is well established (22). Electrocardiographic (ECG) analysis of each of the engrafted CXMD dogs were therefore performed immediately prior to sacrifice. Fig. 4 shows a representative record; this ECG was recorded from the animal sacrificed 10 wk after engraftment. The 12-lead ECG from this animal was normal, and no premature complexes or conduction distur-

bances were detected. The strip record demonstrated a sinus rhythm typical for anesthetized dogs (23), indicating that the presence of fetal cardiomyocyte grafts does not appear to induce overt arrhythmia in the canine model.

Discussion

Cardiac dysfunction is frequently associated with loss of myocardial mass. The ability to increase the number of functional cardiomyocytes in a diseased heart would thus have potential therapeutic value. The experiments presented here demonstrate that fetal cardiomyocytes can form stable grafts in the adult canine heart. Engrafted donor cells were observed to be tightly juxtaposed and well aligned with host cardiomyocytes. Connexin43 immunoreactivity was detected by confocal microscopy at junctional complexes between donor and host cells, indicating (within the limits of the assay) the formation of gap junctions. The presence of fetal cardiomyocyte grafts did not induce overt arrhythmia in the canine experiments. Cellular engraftment can thus successfully augment cardiomyocyte number in the adult canine heart. Ultrastructural analysis of analogous experiments with mice revealed the presence of complete intercalated discs between donor and host cardiomyocytes. Collectively, these results raise the possibility that engraftment of fetal cardiomyocytes might provide a mechanism to augment myocardial function in large animals.

The canine grafting experiments utilized the dystrophin gene product as a marker with which to follow the fate of donor cardiomyocytes. The utility of dystrophin as a cell fate marker was initially established using donor cells from MHC-nLAC transgenic mice and dystrophic mdx hosts. All graft cardiomyocytes which exhibited βGAL activity also expressed dystrophin. Nonetheless, it is important to recognize that some studies have been hampered by the appearance of dystrophin immunoreactivity in control dystrophic skeletal and cardiac muscle (9, 24). It was suggested that the appearance of anti-dystrophin immunoreactivity might be due in part to the extreme size of the dystrophin structural gene. The stochastic accumulation of additional mutations within the gene, while insufficient to rescue dystrophin function, might be sufficient to generate a gene product recognized by some anti-dystrophin antibodies. Fetal cardiomyocyte grafts in the CXMD hearts were initially screened with

Table II. Summary of Fetal Canine Cardiomyocyte Grafts

Animal	Age of graft	Injection area	Number injections	Cells/injection	Blocks/site	Blocks with DYS ⁺ cells*	
						CAP 6–10	DYS1
1	2.5 w	a	1	10 ⁶	1	1/1	1/1
		b	1	10 ⁵	1	1/1	1/1
		c	1	10 ⁴	1	1/1	ND
2	4.5 w	a	13 [‡]	10 ⁴	2	2/2	1/1
		b	13 [‡]	10 ⁴	2	2/2	2/2
3	10 w	a	10 [‡]	10 ⁴	1	1/1	1/1
		b	10 [‡]	10 ⁴	1	2/2	1/1

* Grafts were scored positive if immunoreactivity was detected with the DYS1 and/or CAP 6–10 antibodies. In instances where multiple injections were performed, parallel tracts of dystrophin positive cells could frequently be detected. No DYS1 immunoreactivity was detected in control myocardial regions (right ventricular wall), or in samples of muscle isolated from nonengrafted controls (three independent animals). [‡] Injections were localized to a linear array of ~3 cm.

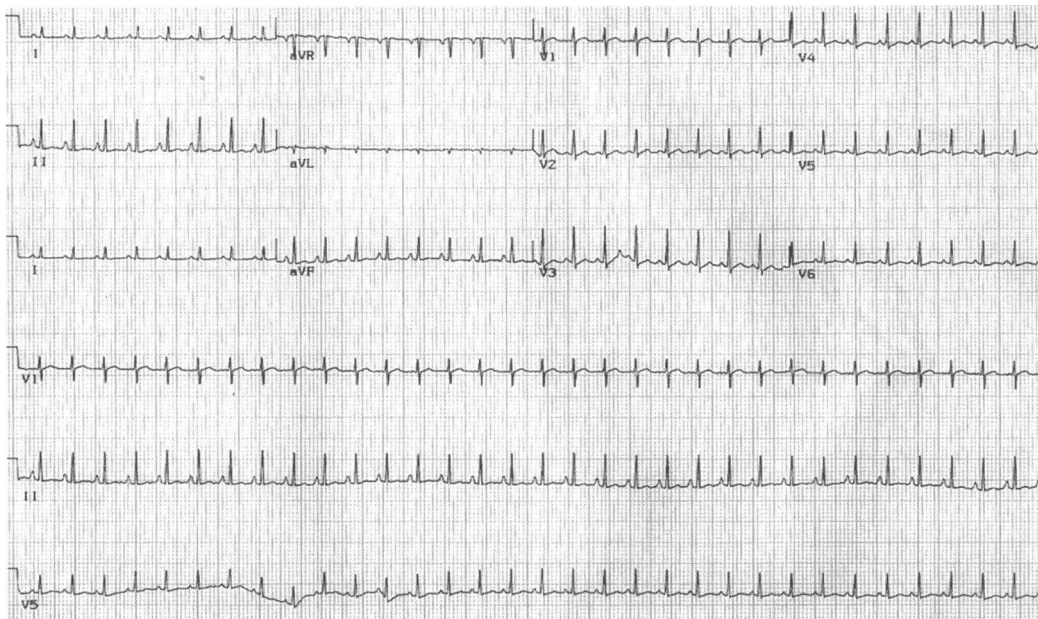


Figure 4. ECG analysis of engrafted CXMD hearts. A representative 12-lead electrocardiograph (ECG) of a CXMD dog recorded 10 wk after engraftment. Note the absence of premature complexes and conduction disturbances.

CAP 6–10, a relatively high affinity polyclonal anti-dystrophin antibody raised against the rod domain of the molecule (amino acid residues 1991–3112). Given the potential caveat of “immunoreactive reversions” raised above, graft formation in CXMD hosts was confirmed on adjacent sections with a second antibody, DYS1, a slightly lower affinity anti-dystrophin monoclonal antibody which recognizes a different epitope (amino acid residues 1181–1388). No DYS1 immunoreactivity was observed in multiple sections of three control CXMD samples (Table II). Given the unequivocal nature of the DYS1 control experiment, the signal observed in experimental animals indisputably indicates the presence of engrafted fetal cardiomyocytes. This view was further substantiated by anti-utrophin immunohistology, which provided a second, albeit negative, marker for the engrafted fetal cardiomyocytes.

The results presented here indicate that cellular grafting can successfully augment cardiomyocyte number in the hearts of adult dogs. Despite the promise of these initial experiments, a number of issues must be satisfactorily addressed before the therapeutic potential of cellular engraftment can be realized. Clearly the most important caveat is to establish the functional competence of engrafted cardiomyocytes. Although this issue was not directly addressed in the current study, evidence supporting the notion that the engrafted cells were functionally coupled was obtained. Ultrastructural analysis clearly indicated the presence of complete intercalated discs between host and donor cardiomyocytes in the murine model. Modification of the fixation procedure permitted the unambiguous identification of gap junctions in the current study. Thus the requisite structures for both action potential and contractile force propagation between donor and host cardiomyocytes are present in the engrafted hearts. The presence of appropriately localized connexin43 immunoreactivity suggested that a similar degree of physical coupling may also occur in the canine grafts. Importantly, graft cardiomyocyte sarcomeres were observed to be aligned and in register with those in host cardiomyocytes, consistent

with their participation in a functional syncytium. Definitive assessment of functional coupling between donor and host cardiomyocytes will be dependent upon the localization of donor cardiomyocytes with a vital dye which can be exploited in conjunction with electrophysiologic and/or contractile assays. Unfortunately, none of the vital β GAL dyes tested worked sufficiently well with intact live tissue to enable us to identify engrafted regions.

Several other issues must be addressed when considering the potential of therapeutic cellular grafting. The current study demonstrated that fetal cardiomyocyte grafts did not induce overt cardiac arrhythmia in the canine model. Indeed, 12 lead ECGs recorded from engrafted animals were indistinguishable from controls. Although previous studies failed to detect graft-induced arrhythmia in murine experiments (5), the significance of those observations was equivocal given the relative resistance of this species to arrhythmogenic episodes. The absence of conduction abnormalities in engrafted canine hearts is thus an important observation. Despite this favorable preliminary result, additional experiments are needed to determine if the graft-myocardium border acts as a predisposing substrate for arrhythmia. Long term screening with Holter monitors would provide additional information regarding any arrhythmogenic propensity resulting from the grafting procedure.

As indicated above, successful rescue of damaged myocardium will require donor myocyte seeding at a sufficiently high density to impact on myocardial function. Although relatively high seeding densities were observed in the present study (an average value of 37% was obtained, see Table I), quantitative morphometric analyses to ascertain the absolute graft area were not performed. Prudence dictates that the variables which ultimately will impact upon donor cell seeding density be addressed prior to the initiation of comprehensive morphometric studies. Towards that end, initial studies indicated that varying either the number of cells per injection or the number of injections per unit area did not negatively affect the ability to form grafts.

Additional experiments aimed at refining these variables will undoubtedly result in optimization of the ensuing graft size. It is nonetheless encouraging to note that grafts spanning as much as 2 mm of the host myocardium were observed in the present study. Although the number of injections per unit area which the myocardium can tolerate remains to be established, human skeletal muscle has tolerated an array of 100 injections in a 24 cm² area (9). If optimization of the myocardial injection protocol resulted in the consistent generation of grafts in excess of 2 mm, delivery of donor cardiomyocytes in a similar array might significantly impact on cardiac function. Without knowledge of the ultimate number of injections per unit area required for functional augmentation, one cannot predict what conditions may be treatable by intracardiac grafting. In the case of global cardiomyopathies, effective treatment of the entire heart may not be feasible. However localized treatment might be useful in cases such as myocardial infarction, where the diseased tissue is regionally restricted.

Another important consideration is the availability of suitable donor cells. Although difficulties may be encountered in procuring sufficient numbers of primary human fetal cells for engraftment, amplification of fetal cardiomyocyte explants in vitro might facilitate the banking of donor cells. Such approaches would be dependent upon the continued identification and functional analysis of cardiomyocyte cell cycle regulatory proteins (reviewed in 28), as well as exploitation of currently available in vitro gene transfer techniques. Identification of the cardiomyocyte lineage determining gene(s) could provide an alternative source of donor cardiomyocytes (reviewed in 29). Transfection of one (or several) determining genes into an appropriately permissive cell may result in the genesis of donor cardiomyocytes in vitro (as is currently possible for skeletal myogenesis). Cardiogenic induction is also possible with embryonic stem cells isolated from mice (30), rats and rabbits. Generation of an equivalent human cell line would provide yet another source of potential donor cells. Chronic immune suppression would likely be required to maintain most types of intracardiac grafts, as is currently required for whole organ transplant.

The apparent plasticity of the dystrophic myocardium deserves comment. The degree of donor cell integration in both the mdx and CXMD models appeared superior to that observed previously with non-dystrophic hosts (5). Although this observation is presently only phenomenological in nature, it is nonetheless important to consider to what extent the absence of dystrophin may influence donor cardiomyocyte integration. Dystrophin is thought to provide a link between the myocyte actin cytoskeleton and the extracellular environment. Since dystrophin is localized along the cytoplasmic face of the plasma membrane (reviewed in 25), extracellular linkage would require the participation of a membrane spanning structure. The dystrophin-glycoprotein complex, a structure comprised of five dystrophin-associated proteins (26), is thought to provide linkage between dystrophin and the extracellular matrix. Expression of these dystrophin-associated proteins is markedly reduced in dystrophic muscle from Duchenne patients, mdx mice and CXMD dogs (reviewed in 27). Given that the dystrophin-glycoprotein complex undoubtedly influences myocyte-matrix interactions (and by extension myocyte-myocyte interaction), the apparent superior integration of donor cells in the mdx and CXMD myocardium might simply reflect intrinsic differences

in cell-cell and/or cell-extracellular matrix interactions in dystrophic versus normal myocardium.

In summary, the experiments reported here establish that fetal cardiomyocyte grafting can readily be extended to the canine myocardium, and that the presence of intracardiac grafts does not overtly disrupt the normal autonomic function of the host heart. Additional experiments are required to optimize graft size and to establish the presence of functional donor-host coupling in the canine model. Once these goals are realized, the efficacy of fetal cardiomyocyte engraftment in a diseased myocardium can be examined rationally.

Acknowledgments

We thank Tim Byers (Indiana University) for the gift of anti-dystrophin antibody CAP 6-10, Brian Patton (Kranert Institute) for help with the confocal microscopy, and Gerald Wertheim and Jake Rohleder (Kranert Institute) for expert technical assistance.

This work was supported by grants from the NHLBI (L. J. Field). This work was done during the tenure of an Established Investigatorship from the American Heart Association (L. J. Field). G. Y. Koh was supported by a Grant in Aid from the American Heart Association, Indiana Affiliate, and M. G. Klug was supported by a predoctoral fellowship from the American Heart Association, Indiana Affiliate. B. J. Cooper was supported by a grant from the Muscular Dystrophy Association.

References

1. Koh, G. Y., M. H. Soonpaa, M. G. Klug, and L. J. Field. 1993. Long-term survival of AT-1 cardiomyocyte grafts in syngeneic myocardium. *Am. J. Physiol.* 264:H1727-1733.
2. Koh, G. Y., M. G. Klug, M. H. Soonpaa, and L. J. Field. 1993. Differentiation and long-term survival of C2C12 myoblast grafts in heart. *J. Clin. Invest.* 92:1548-1554.
3. Zibaitis, A., D. Greentree, F. Ma, D. Marelli, M. Duong, and R. C.-J. Chiu. 1994. Myocardial regeneration with satellite cell implantation. *Transplant. Proc.* 26:3294.
4. Robinson, S. W., P. C. Cho, M. A. Acker, and P. D. Kessler. 1994. Arterial delivery of skeletal myoblasts to the heart. *J. Cell. Biochem.* 18D, 531 (Abstr.).
5. Soonpaa, M. H., G. Y. Koh, M. G. Klug and L. J. Field. 1994. Formation of nascent intercalated discs between grafted fetal cardiomyocytes and host myocardium. *Science (Wash. DC)*. 264:98-101.
6. Morgan, J. E., D. J. Watt, J. C. Sloper, and T. A. Partridge. 1988. Partial correction of an inherited biochemical defect of skeletal muscle by grafts of normal muscle precursor cells. *J. Neuro. Sci.* 86:137-147.
7. Watt, D. J., J. E. Morgan, and T. A. Partridge. 1984. Use of mononuclear precursor cells to insert allogeneic genes into growing mouse muscles. *Muscle & Nerve*. 7:741-750.
8. Partridge, T. A., J. E. Morgan, G. R. Coulton, E. P. Hoffman, and L. M. Kunkel. 1989. Conversion of mdx myofibres from dystrophin-negative to -positive by injection of normal myoblasts. *Nature (Lond.)*. 337:176-179.
9. Gussone, E., G. K. Pavlath, A. M. Lancet, K. R. Sharma, R. G. Miller, L. Steinman, and H. M. Blau. 1992. Normal dystrophin transcripts detected in Duchenne muscular dystrophy patients after myoblast transplantation. *Nature (Lond.)*. 356:435-438.
10. Thompson, L. 1992. Cell-transplant results under fire. *Science (Wash. DC)*. 257:472-474.
11. Thompson, L. 1992. Researchers call for time out on cell-transplant research. *Science (Wash. DC)*. 257:738-740.
12. Soonpaa, M. H., and L. J. Field. 1994. Assessment of cardiomyocyte DNA synthesis during hypertrophy in adult mice. *Am. J. Physiol.* 266:H1439-1445.
13. Bullock, G. R., and P. Petrusz. 1983. Techniques in Immunocytochemistry, Vol. II. Academic Press, New York.
14. Cooper, B. J., N. J. Winand, H. Stedman, B. A. Valentine, E. P. Hoffman, L. M. Kunkel, M. O. Scott, K. H. Fischbeck, J. N. Kornegay, R. J. Avery, J. R. Williams, R. D. Schmickel, and J. E. Sylvester. 1988. The homologue of the Duchenne locus is defective in X-linked muscular dystrophy of dogs. *Nature (Lond.)*. 334:154-156.
15. Valentine, B. A., B. J. Cooper, A. de Lahumta, R. O'Quinn, and J. T. Blue. 1988. Canine X-linked muscular dystrophy. An animal model of Duchenne muscular dystrophy: clinical studies. *J. Neurol. Sci.* 88:69-81.
16. Valentine, B. A., B. J. Cooper, J. F. Cummings, and A. de Lahumta. 1990.

- Canine X-linked muscular dystrophy: morphologic lesions. *J. Neurol. Sci.* 97:1–23.
17. Valentine, B. A., N. J. Winand, D. Pradhan, N. S. Noise, A. de Lahunta, J. N. Kornegay, and B. J. Cooper. 1992. Canine X-linked muscular dystrophy as an animal model of Duchenne muscular dystrophy. *Am. J. Med. Genet.* 42:352–356.
 18. Matsumura, K., J. M. Ervasti, K. Ohlendieck, S. D. Kahl, and K. P. Campbell. 1992. Association of dystrophin-related protein with dystrophin-associated proteins in mdx mouse muscle. *Nature (Lond.)*. 360:588–591.
 19. Mizuno, Y., I. Nonaka, S. Hirai, and E. Ozawa. 1993. Reciprocal expression of dystrophin and utrophin in muscles of Duchenne muscular dystrophy patients, female DMD-carriers and control subjects. *J. Neuro. Sci.* 119:43–52.
 20. Sahashi, K., T. Ibi, H. Suoh, N. Nakao, M. Tashiro, K. Marui, K. Arahat, and H. Sugita. 1994. Immunostaining of dystrophin and utrophin in skeletal muscle of dystrophinopathies. *Int. Med.* 33:277–283.
 21. Beyer, E. C., D. L. Paul, and D. A. Goodenough. 1987. Connexin43: a protein from rat heart homologous to a gap junction protein from liver. *J. Cell Biol.* 105:2621–2629.
 22. Antzelevitch, C., S. Sicouri, S. H. Litovsky, A. Lukas, S. C. Krishnan, J. M. DiDiego, G. A. Gintant, and D. W. Liu. 1991. Heterogeneity within the ventricular wall. Electrophysiology and pharmacology of epicardial, endocardial and M cells. *Circ. Res.* 69:1427–1429.
 23. Zipes, D. P. 1990. Influence of myocardial ischemia and infarction on autonomic innervation of heart. *Circulation.* 82:1095–1105.
 24. Danko, I., V. Chapman, and J. A. Wolff. 1992. The frequency of revertants in mdx mouse genetic models for Duchenne muscular dystrophy. *Pediatric Res.* 32:128–131.
 25. Cullen, M. J., and S. C. Watkins. 1993. Ultrastructure of muscular dystrophy: new aspects. *Micron.* 24:287–307.
 26. Ervasti, J. M., and K. P. Campbell. 1991. Membrane organization of the dystrophin-glycoprotein complex. *Cell.* 66:1121–1131.
 27. Matsumura, K., and K. P. Campbell. 1994. Dystrophin-glycoprotein complex: its role in the molecular pathogenesis of muscular dystrophies. *Muscle and Nerve.* 17:2–15.
 28. Daud, A. I., and L. J. Field. 1993. Interaction between host proteins and SV40 Large T-Antigen in transformed cardiomyocytes. *Heart Failure.* 9:183–198.
 29. Olson, E. N. 1993. Regulation of muscle transcription by the MyoD family. The heart of the matter. *Circ. Res.* 72:1–6.
 30. Doetschman, T. C., H. Eistetter, M. Katz, W. Schmidt, and R. Kemler. 1985. The in vitro development of blastocyst-derived embryonic stem cell lines: formation of visceral yolk sac, blood islands and myocardium. *J. Embryol. Exp. Morph.* 87:27–45.